

This is a repository copy of *Development of a new pan-European testate amoeba transfer function for reconstructing peatland palaeohydrology*.

White Rose Research Online URL for this paper:

<https://eprints.whiterose.ac.uk/106752/>

Version: Accepted Version

Article:

Amesbury, Matthew J., Swindles, Graeme T., Bobrov, Anatoly et al. (10 more authors) (2016) Development of a new pan-European testate amoeba transfer function for reconstructing peatland palaeohydrology. *Quaternary Science Reviews*. pp. 132-151. ISSN 0277-3791

<https://doi.org/10.1016/j.quascirev.2016.09.024>

Reuse

This article is distributed under the terms of the Creative Commons Attribution (CC BY) licence. This licence allows you to distribute, remix, tweak, and build upon the work, even commercially, as long as you credit the authors for the original work. More information and the full terms of the licence here:

<https://creativecommons.org/licenses/>

Takedown

If you consider content in White Rose Research Online to be in breach of UK law, please notify us by emailing eprints@whiterose.ac.uk including the URL of the record and the reason for the withdrawal request.

1 Development of a new pan-European testate amoeba transfer 2 function for reconstructing peatland palaeohydrology

3
4 Matthew J. Amesbury^{1*}, Graeme. T. Swindles², Anatoly Bobrov³, Dan J. Charman¹,
5 Joseph Holden², Mariusz Lamentowicz⁴, Gunnar Mallon⁵, Yuri Mazei^{6,7}, Edward A. D.
6 Mitchell⁸, Richard J. Payne^{6,9}, Thomas P. Roland¹, T. Edward Turner² and Barry G.
7 Warner¹⁰

8
9 * Corresponding author: Email: m.j.amesbury@exeter.ac.uk; Phone: +44(0)1392 725892; Fax:
10 +44(0)1392 723342 (M. J. Amesbury).

11
12 ¹ Geography, College of Life and Environmental Sciences, University of Exeter, UK.

13 ² water@leeds, School of Geography, University of Leeds, UK.

14 ³ Faculty of Soil Science, Lomonosov Moscow State University, Russia.

15 ⁴ Laboratory of Wetland Ecology and Monitoring & Department of Biogeography and Palaeoecology,
16 Faculty of Geographical and Geological Sciences, Adam Mickiewicz University, Poland.

17 ⁵ Department of Geography, University of Sheffield, UK.

18 ⁶ Department of Zoology and Ecology, Penza State University, Russia.

19 ⁷ Department of Hydrobiology, Lomonosov Moscow State University, Russia

20 ⁸ Institute of Biology, Faculty of Science, University of Neuchâtel, Switzerland.

21 ⁹ Environment, University of York, UK.

22 ¹⁰ Earth and Environmental Sciences, University of Waterloo, Canada.

23
24 **Author contributions:** MJA and GTS conceived the work, compiled the data, conducted data analysis
25 and wrote the manuscript. All other authors contributed data, actively discussed the direction of the
26 research, developed the approach to taxonomic harmonisation and/or contributed to manuscript
27 editing.

28 29 **Abstract**

30 In the decade since the first pan-European testate amoeba-based transfer function for peatland
31 palaeohydrological reconstruction was published, a vast amount of additional data collection has
32 been undertaken by the research community. Here, we expand the pan-European dataset from 128
33 to 1799 samples, spanning 35° of latitude and 55° of longitude. After the development of a new
34 taxonomic scheme to permit compilation of data from a wide range of contributors and the removal
35 of samples with high pH values, we developed ecological transfer functions using a range of model
36 types and a dataset of ~1300 samples. We rigorously tested the efficacy of these models using both
37 statistical validation and independent test sets with associated instrumental data. Model
38 performance measured by statistical indicators was comparable to other published models.
39 Comparison to test sets showed that taxonomic resolution did not impair model performance and
40 that the new pan-European model can therefore be used as an effective tool for palaeohydrological
41 reconstruction. Our results question the efficacy of relying on statistical validation of transfer
42 functions alone and support a multi-faceted approach to the assessment of new models. We
43 substantiated recent advice that model outputs should be standardised and presented as residual

44 values in order to focus interpretation on secure directional shifts, avoiding potentially inaccurate
45 conclusions relating to specific water-table depths. The extent and diversity of the dataset
46 highlighted that, at the taxonomic resolution applied, a majority of taxa had broad geographic
47 distributions, though some morphotypes appeared to have restricted ranges.

48

49 **Keywords:** Testate amoeba, peatland, water table, transfer function, Europe, spatial scale, data
50 compilation, taxonomy.

51

52 **Highlights**

- 53 • A vastly expanded dataset of European peatland testate amoeba samples is compiled;
- 54 • A new taxonomic scheme is developed to facilitate data compilation;
- 55 • Palaeohydrological transfer functions are tested statistically and against independent data;
- 56 • The new model is an effective tool for palaeohydrological reconstruction across Europe;
- 57 • Model outputs should be standardised and presented as residual values.

58

59 **Introduction**

60 Testate amoebae are microscopic, unicellular shelled protozoa that are abundant in a range of
61 wetlands, including peatlands (Mitchell et al., 2008). Early research demonstrated the close
62 ecological coupling between testate amoebae and hydrological parameters such as water-table
63 depth and moisture content in such environments (e.g. Jung, 1936; Schönborn, 1963). Quantitative
64 ecological approaches demonstrated the strength of this relationship and used it to derive
65 reconstructions of hydrological variability from fossil testate amoebae (Warner and Charman, 1994;
66 Woodland et al., 1998). This approach has subsequently been thoroughly developed and extended
67 geographically, using more advanced statistical techniques (e.g. Charman et al., 2007; Booth, 2008;
68 Swindles et al., 2009, 2014, 2015a; Amesbury et al., 2013). Testate amoeba-based hydrological
69 reconstructions are now frequently used as hydroclimate proxies in studies of Holocene climate
70 change (e.g. Charman et al., 2006; Swindles et al., 2010; Elliott et al., 2012; Lamentowicz et al., 2015;
71 Willis et al., 2015). Central to such research is typically the application of a transfer function. These
72 statistical models apply the observed modern ecological preferences of amoebae via a range of
73 mathematical approaches (Juggins and Birks, 2011) to fossil assemblages to quantitatively
74 reconstruct environmental variables of interest, primarily water-table depth in ombrotrophic
75 peatlands, but occasionally other parameters such as pH (Markel et al., 2010; Mitchell et al., 2013).
76 Testate amoeba-based hydrological transfer functions have now been developed in a wide range of
77 locations (e.g. Li et al., 2015; Swindles et al., 2015a, 2014; van Bellen et al., 2014) and wetland types,
78 primarily in bogs, but also in fens (Payne, 2011; Lamentowicz et al., 2013a; Lamentowicz et al.,
79 2013b). Recent debates in this field have focussed on 1) more rigorous analysis of transfer function
80 results, whether via statistical testing (Telford and Birks, 2005, 2009, 2011a, 2011b, Payne et al.,
81 2012, 2016; Amesbury et al., 2013), or by comparison with instrumental data (Swindles et al.,
82 2015b); 2) the appropriateness of varying spatial scales for transfer function development (Turner et
83 al., 2013); and 3) the validity of applying models outside of the geographic range over which they
84 were developed (Turner et al., 2013; Willis et al., 2015), and hence the cosmopolitanism of testate
85 amoeba ecological preferences (Booth and Zygmunt, 2005) across a range of geographical locations
86 (Smith et al., 2008).

87

88 When transfer function models developed in one region are applied in a different region where no
89 local model exists, results may theoretically be undermined by a number of factors. These include
90 missing modern analogues, differences in testate amoeba ecology or biogeography between the two
91 regions (Turner et al., 2013), the technique used to measure water-table depth in the calibration
92 data sets (Markel et al., 2010; e.g. long-term mean versus one-off measurement), regionally diverse
93 seasonal variability (Sullivan and Booth, 2011; Marcisz et al., 2014) or vertical zonation (van Bellen et
94 al., 2014) of testate assemblages, or local-scale variability in the response of certain taxa, or even
95 communities, of testate amoebae to environmental variables (e.g. Booth and Zygmunt, 2005).
96 However, in practice, when transfer functions from one region are applied to fossil data from a
97 separate region, even over distances of thousands of kilometres (Turner et al., 2013; Willis et al.,
98 2015), or when regional- and continental-scale models are compared (e.g. Amesbury et al., 2008;
99 Charman et al., 2007; Swindles et al., 2009; Turner et al., 2013), it is largely only the absolute values
100 and magnitude of reconstructed water-table shifts that vary between models, with the timing and
101 direction of change being generally consistent. Given that the absolute values and magnitude of
102 transfer function-reconstructed change in water-table depth have recently been questioned by
103 direct comparison of reconstructed and instrumental water-table depths (Swindles et al., 2015b), it
104 could be argued that a) testate amoeba-based transfer function reconstructions should be viewed as
105 semi-quantitative and interpretation should be based only on the timing and direction of change;
106 and that b) the general ecological cosmopolitanism of testate amoebae (e.g. Mitchell et al., 2000;
107 Booth and Zygmunt, 2005) when studied at coarse taxonomic level (i.e. morphotypes – but see
108 Heger et al., 2013 for an example of cryptic diversity showing geographical patterns) means that
109 regional transfer functions are widely applicable, at least at an intra-continental or even intra-
110 hemispheric scale.

111

112 Approaching a decade after the publication of the first testate amoeba-based pan-European transfer
113 function (Charman et al., 2007), which included 128 samples from seven countries, we present a
114 new collaborative effort to vastly extend that dataset, including both published and unpublished
115 data that increases the number of samples to 1799, from a much expanded geographical range
116 covering 18 countries spaced over 35° of latitude and 55° of longitude. In doing so, we develop a
117 new transfer function for peatland testate amoeba palaeohydrological reconstruction and shed new
118 light on the biogeography and cosmopolitanism of testate amoebae and the potential effects of
119 varying spatial scales and supra-regional application on resulting transfer function reconstructions.
120 We rigorously test our newly developed models using a novel combination of statistical validation
121 and checks against independent testate amoeba data with associated instrumental water-table
122 depth measurements. Ultimately, we aim to facilitate more reliable comparisons of spatial and
123 temporal patterns of peatland-derived palaeoclimate records at a continental scale.

124

125 **Methods**

126

127 *Data compilation and taxonomy*

128 We compiled a full dataset containing 1799 samples from 113 sites in 18 countries from 31
129 published studies, with contributions of unpublished data from two countries (Table 1; Figure 1). All
130 samples in the dataset had an associated water-table depth value, whereas a reduced number
131 (n=1564) also had an associated pH value.

132

133 [INSERT FIGURE 1]

134 **Figure 1:** Site locations (see Table 1 for more site details). Sites are coloured by eco-region: Atlantic =
135 red, Scandinavia = green; Continental = blue. For reference to colour, readers are referred to the
136 online version of this article.

137

138

139 Although the potential risks of taxonomic inconsistency, especially in large data compilations with
140 large numbers of analysts, are clear (Payne et al., 2011), the likely effect of using a low taxonomic
141 resolution potentially decreased model performance (in statistical terms) rather than any effect on
142 the timing or direction of major changes in wetness (Mitchell et al., 2014). Due to the high number
143 of data contributors/analysts in this compilation and in order to ensure taxonomic consistency
144 across the merged dataset, we adopted a low-resolution approach to defining an appropriate
145 taxonomic scheme, merging morphologically similar taxa together into a series of newly defined
146 groups. Initial examination of contributed datasets made it clear that different analysts had grouped
147 (or 'lumped') or split taxa to varying extents, with many taxa only present in individual datasets. A
148 low-resolution approach to taxonomy was therefore considered to be not only the most
149 parsimonious, but also the only scientifically valid approach to the compilation of such a large
150 dataset, despite genuine variation in water-table optima occurring between taxa within some new
151 groupings (see Results). Individual analysts should not count new samples in line with the low-
152 resolution taxonomic scheme applied here, but rather differentiate between readily identifiable taxa
153 in line with current taxonomies and group taxa together only for statistical analysis. The majority of
154 recently published papers on peatland testate amoebae use Charman et al. (2000) as a standard
155 identification guide, with an increasing number of variations noted in recent years including, most
156 prevalently, the reclassification of *Amphitrema flavum* as *Archerella flavum* (Loeblich and Tappan,
157 1961), the splitting out of certain 'type' groupings into their constituent taxa (e.g. *Cyclopyxis*
158 *arcelloides* type into *Cyclopyxis arcelloides sensu stricto*, *Phryganella acropodia* and *Diffflugia*
159 *globulosa*; Turner et al., 2013) and more recent reclassifications based on phylogenetic studies (e.g.
160 *Nebela* taxa moving to the genera *Longinebela*, *Planocarina* and *Gibbocarina*; Kosakyan et al., 2016).

161

162 Across all 1799 samples in the full dataset, a total of 186 individual taxa were identified, with the
163 final taxonomic scheme containing a reduced 60 taxa, of which 41 were 'type' groupings (38 newly
164 defined) that each contained between two and 11 taxa with similar morphological features (Table 2).
165 These groups were defined with reference to a range of identification keys and source literature
166 (Cash and Hopkinson, 1905, 1909, Cash et al., 1915, 1918; Ogden and Hedley, 1980; Meisterfeld,
167 2000a, 2000b) as well as using the expertise and experience of the authors. Our treatment of the
168 two *Euglypha* groups – *E. ciliata* type and *E. rotunda* type – provides an example of the low
169 resolution approach we adopted. These groups contained 11 and eight individual taxa respectively
170 that had been identified by individual analysts in the originally contributed datasets. However, the
171 only morphological characteristic that we could identify as consistently applied across all datasets
172 was size, with several datasets only defining *E. tuberculata* (i.e. larger type >45 µm) and *E. rotunda*
173 (i.e. smaller type <45 µm). Since the presence/absence of spines (e.g. *E. strigosa* vs. *E. tuberculata*)
174 may be biased by taphonomic processes (Payne et al., 2011), we therefore defaulted to a two-taxon
175 system for this family.

176

177 When all data were compiled using this new taxonomy, taxa which occurred in <18 samples (i.e. 1%
178 of the data) were excluded as rare taxa (n=8; Table 3), resulting in a total of 52 taxa in the 'edited'
179 dataset. With the exception of *Cyphoderia* sp., *Placocista* sp. and *Trigonopyxis* sp., which were
180 included in *Cyphoderia ampulla* type, *Placocista spinosa* type and *Trigonopyxis arcua* type
181 respectively (groupings which contained all potential examples of these genera), all individuals
182 defined only to the family level were also excluded from the dataset. Where this process resulted in
183 a total assemblage <90% of the original total count, we excluded whole samples from the full
184 dataset (n=24, Table 4), resulting in a total of 1775 samples in an 'edited' dataset (Figure 2). Transfer
185 function development proceeded from this 'edited' dataset. Hereafter, this 'edited' dataset will be
186 referred to as the full dataset.

187

188 [INSERT FIGURE 2]

189 **Figure 2:** Percentage distribution of all taxa. Taxa are ordered from 'wet' on the left to 'dry' on the
190 right based on the taxa optima from the WA-Tol (inv) model of the full dataset (n = 1775).

191

192

193 *Statistics*

194 Since the full dataset contained samples from a range of different peatland types on a continuum
195 between more oligotrophic bogs to more eutrophic fens (range in pH values of 2.5 – 8.1), and in light
196 of the overarching aim of this study to produce a transfer function for palaeohydrological
197 reconstruction, we initially used exploratory ordination analyses (non-metric multidimensional
198 scaling (NMDS) using the Bray-Curtis dissimilarity) to objectively reduce the dataset to those samples
199 more representative of the nutrient poor, ombrotrophic peatlands commonly used in palaeoclimate
200 research. We applied a high pH cut-off based on NMDS axis one scores and k-means cluster analysis
201 (for additional details see ordination results). All analyses were carried out in R version 3.2.2 (R Core
202 Team, 2015) using the packages *vegan* (Oksanen et al., 2015) for NMDS and cluster analysis and
203 *pvclust* for significance testing between clusters (Suzuki and Shimodaira, 2014).

204

205 Transfer function development was also carried out in R (R Core Team, 2015) using the package *rioja*
206 (Juggins, 2015), applying four commonly used model types, namely: weighted averaging (WA; with
207 and without tolerance downweighting (WA-Tol)), weighted average partial least squares (WAPLS),
208 maximum likelihood (ML) and the modern analogue technique (MAT). In each case, only results of
209 the best performing (judged by root mean square error of prediction (RMSEP) and R^2) model within
210 each type are shown. RMSEP values were calculated using the standard leave-one-out ($RMSEP_{LOO}$)
211 technique, as well as leave-one-site out ($RMSEP_{LOSO}$; Payne et al., 2012) and segment-wise ($RMSEP_{SW}$;
212 Telford and Birks, 2011b) approaches. Spatial autocorrelation tests were calculated in the R package
213 *palaeoSig* (Telford, 2015) using the 'rne' (random, neighbour, environment) function.

214

215 To test the applicability of the new model, we applied it to 1) downcore independent test data from
216 a long-term (~6000 years) record from Tor Royal Bog (TRB) in Dartmoor, UK (Amesbury et al., 2008),
217 2) a simulated palaeo dataset developed from surface samples with associated automated
218 instrumental water-table depth measurements, ordered to 'create' two major shifts in water-table
219 depth (Swindles et al., 2015b) and 3) downcore independent test data from a short-term record
220 from Männikjärve Bog, Estonia with associated automated instrumental water-table data (Charman
221 et al., 2004). For test sets 2 and 3, we used annual and summer (JJA) mean water-table depth values

222 in each case, calculated from multiple daily measurements (for full details see source publications).
223 Sample-specific errors for the transfer function reconstructions were based on 1000 bootstrapping
224 cycles. We compared our reconstructions with output from the previous European transfer function
225 (Charman et al., 2007) and tested the significance of the new reconstructions using the 'randomTF'
226 function in palaeoSig (Telford, 2015).

227

228 We used the programme PAST (version 3.10; Hammer et al., 2001) to run one-way PERMANOVA
229 tests (9999 iterations) of the differences between samples from different countries and three
230 assigned eco-regions (Atlantic, n=461; Scandinavia, n=341; Continental, n=500; Figure 1) that
231 represented broadly different climate zones and degrees of oceanicity/continentality.

232

233 **Results**

234 *Ordination*

235 NMDS of the full dataset (n=1775; Figure 3A and B) showed that the primary environmental variable
236 explaining species distribution along axis 1 was pH, as opposed to water-table depth, illustrating the
237 influence of the peatland type gradient (i.e. ombrotrophic to minerotrophic). A distinct group of
238 samples formed an outlying cluster with high NMDS axis 1 scores. To determine an appropriate pH
239 cut-off to reduce the dataset to those containing nutrient poor, ombrotrophic peatlands, we used
240 results of k-means cluster analysis, forcing the data into two clusters (Figure S1; i.e. lower pH values
241 in Group 1, higher pH values in Group 2). 5.4 was the highest pH where the majority of samples fell
242 in Group 1 and 5.5 was the lowest pH where the majority of samples fell in Group 2. We therefore
243 removed all samples with pH \geq 5.5. This division was supported by plotting NMDS scores against pH,
244 which showed an abrupt jump to higher axis 1 values at this point in the pH range (Figure S1) and
245 also by general peatland ecology: *Sphagnum* moss, the dominant peat-forming species in Northern
246 Hemisphere ombrotrophic peatlands is known to actively acidify its environment (van Breemen,
247 1995) and therefore ombrotrophic bogs are typically dominated by pH ranges of 3.0 – 4.5, with
248 *Sphagnum*-dominated poor fens having marginally higher pH (4.5 – 5.5; Lamentowicz and Mitchell,
249 2005). Using this cut-off resulted in the removal of 370 samples with pH values 5.5 – 8.1 and the
250 removal of all samples from France, Greece and Israel. We re-ran NMDS ordination on the reduced,
251 low-pH dataset (n=1405, including samples without a pH measurement (n=211); Figure 3C and D)
252 which then showed that water-table depth was the primary environmental variable explaining
253 species variation along axis 1 (p<0.001 using the 'envfit' function in vegan), providing a statistical
254 foundation to proceed with transfer function development. Despite water-table depth being the
255 primary explanatory variable after removal of high pH samples, there is still considerable variability
256 along NMDS axis two (Figure 3D) that reflects previous axis one variability (Figure 3B), potentially
257 driven by samples without pH values that may in reality be from sites with pH \geq 5.5. In particular, a
258 group of nine taxa (*Tracheleuglypha dentata* type, *Gibbocarina (Nebela) penardiana* type, *Arcella*
259 *gibbosa* type, *Quadrulella symmetrica*, *Microclamys patella*, *Lesquereusia spiralis* type, *Cyphoderia*
260 *ampulla* type, *Arcella dentata* type and *Pyxidicula operculata* type) fall outside of the main cluster of
261 variability with more negative axis two scores (Figure 3D), potentially suggesting that these taxa may
262 be less reliable water table indicators, associated more with nutrient enrichment (Payne, 2011;
263 Lamentowicz et al., 2013a). Following the removal of high pH samples, all nine are relatively rare
264 taxa, occurring in < 5% of the 1405 samples. Five of the taxa are defined as rare based on previously
265 defined criteria (i.e. < 1% of the dataset, or n=14; *A. dentata* type, *C. ampulla* type, *L. spiralis* type,
266 *M. patella*, *P. operculata* type) and so these were excluded from further analyses, reducing the

267 number of taxa in the dataset for transfer function development to 47. The number of samples in
268 which the remaining four taxa (*A. gibbosa* type, *G. (N.) penardiana* type, *Q. symmetrica*, *T. dentata*
269 type) were present was reduced by > 50% in all cases with the removal of high pH samples (e.g. by
270 52% for *A. gibbosa* type but up to a reduction of > 80% for *Q. symmetrica*), so water-table depth
271 reconstructions based on fossil assemblages containing significant proportions of these taxa should
272 be treated with caution.

273

274 [INSERT FIGURE 3]

275 **Figure 3:** NMDS plots before (A and B) and after (C and D) the removal of samples from the dataset
276 with high pH values. A and C show sample positions, coded by country. B and D show taxa positions
277 for same data as in A and B (but note different axis lengths). Vectors on all plots show influence of
278 environmental drivers. Some taxa positions in B and D have been marginally altered to improve
279 legibility of the figure, but relative positions remain intact. Full names for species abbreviations can
280 be found in Table 2. For reference to colour, readers are referred to the online version of this article.

281

282

283 *Transfer function development and statistical assessment*

284 Before proceeding with transfer function development, we removed 12 further samples with
285 extreme measured water table values (Table S1), resulting in a dataset for transfer function
286 development of 1393 samples. These 12 samples fell below the 0.5th (i.e. representing deep surface
287 ponding, n=2) and above the 99.5th (i.e. representing extreme deep water tables, n=10) percentiles
288 of water-table depth and were removed to avoid the large increase in water-table depth range that
289 would result from their inclusion and the subsequent effect on removal of samples with high
290 residual values. In addition, the removal of extreme deep water-table depth samples is supported by
291 Swindles et al., 2015b, who showed a disconnect between testate amoebae and water table in such
292 circumstances. In keeping with standard practice, we then ran two iterations of models, the first
293 using all samples and the second having removed samples with residual values greater than 20% of
294 the range of water-table values in the dataset (min = -10 cm, max = 85 cm, range = 95 cm, 20% range
295 = 19 cm) (e.g. Amesbury et al., 2013; Booth, 2008; Charman et al., 2007; Payne et al., 2006; Swindles
296 et al., 2009). Residuals removed in the second iteration of model runs were specific to each model
297 type and therefore varied in number (Table 5). The effect of removing residual samples is shown in
298 Figure 4 for the best performing versions of the four model types under investigation (WA-Tol (inv) =
299 weighted average tolerance downweighting with inverse deshrinking; WAPLS C2 = second
300 component of weighted averaging partial least squares; WMAT K5 = weighted mean modern
301 analogue technique with five nearest neighbours). Results for WAPLS C2 are included but fell
302 marginally outside the recommended cut-off for acceptance (5% at $p < 0.05$; Birks, 1998); the second
303 component provided a 4.71% improvement ($p = 0.001$) over the first component (i.e. simple weighted
304 averaging). Residual error plots show that the majority of samples with high residual values fell at
305 the 'dry' end of the water table gradient and that, in general, all models tended to under-predict at
306 the dry end of the gradient (i.e. negative residual value) and over-predict at the wet end of the
307 gradient (i.e. positive residual value). Biplots of observed and predicted water-table depths show
308 that, particularly for both weighted average models and WMAT K5 but not so ML, models tended to
309 reach a plateau of predicted values at around 40 – 50 cm regardless of the observed value. In
310 contrast to previous studies (e.g. Amesbury et al., 2013) which found larger water table tolerances
311 correlated with drier optima, tolerance ranges for the WA-Tol (inv) model were similar throughout

312 the water table gradient (Figure 5), potentially as a result of the ‘averaging out’ effect of taxonomic
313 groupings, although a small group of hydrophilous taxa did have narrower tolerances. The ordering
314 of taxa water table optima (Figure 5) reflected the positioning of taxa along NMDS axis one (Figure
315 3).

316

317 [INSERT FIGURES 4 AND 5]

318

319 **Figure 4:** Biplots of observed and predicted (leave-one-out cross-validated) water-table depth (left)
320 and residual error plots (right) for the best performing versions of the four model types under
321 investigation. WA-Tol (inv) = weighted averaging with tolerance downweighting and inverse
322 deshrinking; WAPLS C2 = second component of weighted averaging partial least squares; WMAT K5
323 = weighted mean modern analogue technique with five nearest neighbours; ML = maximum
324 likelihood. Red points are model runs with all data, black points are model runs after the removal of
325 samples with high residual values. For reference to colour, readers are referred to the online version
326 of this article.

327

328 **Figure 5:** Water-table depth optima and tolerances (cm) for 57 taxa based on the WA-Tol (inv) model
329 after the removal of outlying samples (n=1302).

330

331

332 Performance statistics (Table 5; principally, RMSEP and R^2) before the removal of outlier samples
333 were generally poor, though equivalent to some published models (e.g. Swindles et al., 2015a; van
334 Bellen et al., 2014). After the removal of outlier samples with high residual values (Figure 4),
335 $RMSEP_{LOO}$ values for the WA-Tol (inv), WAPLS C2 and WMAT K5 models fell in the range 7 – 8 cm,
336 equivalent to that generally seen in other published transfer functions (Booth, 2008; Markel et al.,
337 2010; Amesbury et al., 2013; Lamarre et al., 2013; Li et al., 2015; Swindles et al., 2015a) and,
338 notably, similar to the ACCROTELM European model (Charman et al., 2007). $RMSEP_{LOSO}$ values
339 showed a mean relative decrease in performance of only 0.068 (mean of 0.036 without WMAT K5)
340 compared to $RMSEP_{LOO}$, less than that in Payne et al. (2012; mean decrease in performance of
341 0.141). Calculation of $RMSEP_{SW}$ (Figure S2; single value for $RMSEP_{SW}$ is a mean of all individual
342 segment RMSEPs) resulted in a decrease in performance compared to $RMSEP_{LOO}$ for all models with
343 the exception of ML, which supports previous research that found ML outperformed MAT- and WA-
344 based models on unevenly sampled gradients (Telford and Birks, 2011b). There was a prevalence of
345 samples in the water-table depth range 0 – 35 cm, with water-table depths <0 cm and >35 cm less
346 well represented (although it should be noted that due to the high overall number of samples in the
347 dataset, even the lowest frequency segment, 45 – 49.5 cm still contained 15 – 18 samples,
348 depending on model type). Individual segment RMSEP values generally increase where sampling
349 frequency is lower, particularly at the ‘dry’ end of the water table gradient, in keeping with
350 expectation (Telford and Birks, 2011b), except for ML, which shows more consistent RMSEP values
351 across all segments, driving the observed relative improvement in $RMSEP_{SW}$ against other model
352 types. In all cases, RMSEP values, however calculated, remained lower than the standard deviation
353 of all water table measurements (Table 5), suggesting all models have a degree of predictive ability
354 (cf. Amesbury et al., 2013; Mitchell et al., 2013). All models display a degree of spatial
355 autocorrelation (Figure S3), given that r^2 values decline more steeply when geographically proximal,
356 as opposed to random, samples are removed (Telford and Birks, 2009). For all models to some

357 extent, but for WMAT K5 in particular, the decline in r^2 over the first 100 km is similar to the decline
358 for the most environmentally similar samples, indicating that geographically proximal samples are
359 also the most environmentally similar across the dataset. Coupled to the general similarity of R^2
360 from 100 – 1000 km, this reflects the spatial structure of the data whereby each individual data
361 contribution (Table 1) tended to include multiple sites/samples, with individual study locations being
362 widely distributed across Europe (Figure 1).

363

364 *Testing model efficacy*

365 In addition to statistical assessment of model performance, we used three independent data sets,
366 two with associated instrumental water table measurements, to test the new models. Broadly
367 speaking, reconstructions using the four different model types under consideration (WA-Tol (inv),
368 WAPLS-C2, ML, WMAT-K5) showed similar patterns of change to either alternative published
369 transfer function reconstructions or instrumentally recorded water table fluctuations, although
370 water-table depth ranges were more variable (Figure 6). For the Tor Royal Bog test set, all model
371 types reconstructed generally drier conditions and ranges of reconstructed water-table depths were
372 much higher for all model types when compared to a published reconstruction (Figure 6A; Amesbury
373 et al., 2008), particularly for ML. However, when viewed as residual plots (Figure 6B; Swindles et al.,
374 2015b), all models show extremely similar patterns of change over the ~6000 year record. For the
375 simulated shifts in water-table depth (Figure 6C and D; Swindles et al., 2015b), all models again
376 produced comparable reconstructions with the exception of ML. All models reconstructed the
377 simulated shifts in water table with the correct frequency and direction of change, but reconstructed
378 shifts were more abrupt, occurring over 2 – 3 samples, with simulated shifts more gradual, occurring
379 over 6 – 10 samples. Whereas the wet and dry ends of the simulated shifts were single point
380 extremes, modelled reconstructions exhibited more rapid, threshold-type switches in water table
381 interspersed with plateaux of more consistently wet or dry conditions. Reconstructions of monitored
382 water-table depth at Männikjärve fell between the annual and summer mean values for water-table
383 depth (Figure 6E), but when viewed as residual values (Figure 6F), differences were evident in the
384 patterns of change over the c. 50 year record, with the comparatively smooth reconstructions
385 suggesting a broadly drier period during the 1970s and 1985 – 1995, with wetter conditions before
386 and after, whereas instrumental data show that water table varied over shorter time scales
387 throughout the period of monitoring.

388

389 [INSERT FIGURE 6]

390 **Figure 6:** Comparison of transfer function reconstructions from four model types (WA-Tol (inv),
391 WAPLS-C2, ML, WMAT-K5) with independent test sets. A, C & E are raw water-table depth values; B,
392 D & F are residual z-scores. A and B: reconstructions from Tor Royal Bog, Dartmoor, UK (Amesbury et
393 al., 2008) compared (panel A only) with a published reconstruction using a European transfer
394 function (black line; Charman et al., 2007). C and D: reconstructions of simulated wet and dry shifts
395 derived from reordered surface samples with associated instrumental water table measurements
396 (black line = annual mean water-table depth, grey line = summer (JJA) mean water-table depth;
397 Swindles et al., 2015b). Y-axis (not shown) is randomly ordered surface sample codes. E and F:
398 reconstructions of near-surface fossil data from Männikjärve Bog, Estonia with associated long-term
399 instrumental water table measurements (black line = annual mean water-table depth, grey line =
400 summer (JJA) mean water-table depth; Charman et al., 2004). For reference to colour, readers are
401 referred to the online version of this article.

402
403
404
405
406
407
408
409
410
411
412
413
414
415
416
417
418
419
420
421
422
423
424
425
426
427
428
429
430
431
432
433
434
435
436
437
438
439
440
441
442
443
444
445
446

All reconstructions were subject to significance testing against transfer functions built on randomly generated data (Table 6; Telford and Birks, 2011a). This methodology has recently been tested (Payne et al., 2016), with a substantial majority of reconstructions unexpectedly found to be non-significant. In addition, the risks of misapplying (e.g. over-simplified decision making) or over-relying on (e.g. lack of real-world context) p -value cut-offs, are clear (Wasserstein and Lazar, 2016). However, the significance testing technique does provide a method of statistical assessment that can be used as part of a wider toolkit to evaluate model performance. P-values varied between model types and test sets. Only WMAT-K5 reconstructions consistently met the $p < 0.05$ criterion across all test sets. WA-Tol (inv) and WAPLS-C2 reconstructions were consistently $p > 0.05$ though for the Tor Royal Bog and simulated test sets, were consistently $p < 0.08$. ML reconstructions showed the greatest degree of variability, ranging from $p = 0.274$ for the Tor Royal Bog test set to $p = 0.031$ for the Männikjärve test set.

Spatial scales and regional variability

To further investigate the potential effects of varying spatial scales and supra-regional application on resulting transfer function reconstructions, we subdivided our data into three eco-regions (Figure 1); Atlantic ($n=461$), Scandinavia ($n=341$) and Continental ($n=500$). We developed individual transfer functions for each region and applied them to the same three independent test-sets as for the full European-scale models. These three datasets include data from all three eco-regions (Tor Royal Bog in the UK; simulated test set from the UK and Finland; Männikjärve from Estonia) so provide a test of the effects in within- and supra-regional model application (Turner et al., 2013). Given the broad similarity of reconstructions between model types (Figure 6), especially when presented as standardised water-table depth residual values (Swindles et al., 2015b), only one model type (WA-Tol (inv)) was used for this exercise. This model type has been frequently applied in previous studies (e.g. Amesbury et al., 2013; Swindles et al., 2015a, 2009) and in this study, compared favourably to other model types in terms of reported performance statistics, with low $RMSEP_{LOO}$ and $RMSEP_{LOSO}$ values (Table 5). Performance statistics ($RMSEP_{LOO}$, R^2) for the regional models (Table 7) were comparable to, or better than, the full European model (Table 5), potentially suggesting the presence of regional differences in biogeography strong enough to influence model performance. Reconstructed water-table depth profiles for the Atlantic and Continental models for all three independent test sets are broadly similar (Figure 7) and comparable to the WA-Tol (inv) reconstruction using the full European dataset. However, in all three test sets, the Scandinavian model tended to result in notably different profiles. For the Tor Royal Bog and simulated test sets, the Scandinavian model predicted similar patterns of change but overall wetter conditions (Figure 7A and B) whereas for the Männikjärve test set, drier overall conditions were predicted. The Scandinavian model contained the lowest number of samples of all three regions ($n=341$), but still more than many published models. Scandinavian samples also recorded the highest (i.e. wettest) mean water-table depth of the three regional models (Table 7; Figure S4; 12.7 cm compared to 16 cm for the Atlantic and Continental models) and the lowest range of water-table depth values (Table 7; Figure S4; range of 55 cm, compared to 57 cm and 62 cm for the Atlantic and Continental models respectively).

[INSERT FIGURE 7]

447 **Figure 7:** Comparison of three regional transfer function reconstructions to the full European model
448 for the same three independent test sets as Figure 6. All reconstructions use the WA-Tol (inv) model
449 type. A: Tor Royal Bog (black line uses the established ACCROTELM European transfer function of
450 Charman et al., 2007); B: simulated changes in water-table depth (black (annual) and grey (summer)
451 lines are instrumental water table measurements); C: Männikjärve Bog, Estonia (black (annual) and
452 grey (summer) lines are instrumental water table measurements). For reference to colour, readers
453 are referred to the online version of this article.

454
455

456 To provide additional insight into the differences between regional models, we examined the
457 prevalence of individual taxa across the three regions to identify whether taxa were cosmopolitan,
458 or tended to have skewed distributions, favouring a particular region (Figure 8; Figure S5). One-way
459 PERMANOVA tests on both individual countries as well as the three eco-regions showed that there
460 were significant differences between both factor countries and regions ($p < 0.0001$ for both, $F = 29.87$
461 for countries, $F = 45.6$ for regions, assessed by Bray Curtis distance). Twenty-six taxa, including the
462 three most abundant in the dataset (i.e. *Assulina muscorum* ($n = 1180$), *Euglypha ciliata* type
463 ($n = 1145$), *Nebela tincta* type ($n = 1022$)), were evenly distributed across all sub eco-regions within the
464 wider European study zone (Figure S5). However, a large number ($n = 19$) had skewed distributions
465 that suggested taxa were more abundant in particular regions, especially in continental Europe
466 ($n = 14$; Figure 8).

467

468 [INSERT FIGURE 8]

469 **Figure 8:** Taxa with uneven distributions across the three regions ($n = 19$). Taxa with all occurrences
470 $< 5\%$ abundance have been excluded ($n = 2$; DIF GRA and PAR IRR). Region codes on x-axes: 1 =
471 Atlantic, 2 = Scandinavia, 3 = continental Europe. For full taxa abbreviations, see Table 2. Number of
472 occurrences in 1302 samples shown in brackets after taxon code. Red dots indicate complete
473 absence from a particular region. For reference to colour, readers are referred to the online version
474 of this article.

475

476

477 Discussion

478 Data compilation

479 A low-resolution approach to taxonomy was necessitated in this work by the large number of data
480 contributors (see Methods). It has been shown that reducing taxonomic resolution may have a
481 detrimental effect on model performance (Mitchell et al., 2014; as determined by RMSEP and R^2) but
482 with only limited effects on patterns of reconstructed water-table depth. Our data support this view.
483 For example, directional shifts reconstructed by all model types tested showed the same patterns as
484 a European transfer function based on a higher resolution taxonomy (Charman et al., 2007) when
485 applied to a record from Tor Royal Bog, Dartmoor, UK (Figure 6). Particularly when records were
486 standardised (Swindles et al., 2015b) to remove variability in specific reconstructed water-table
487 depth values (Figure 6B), the reconstructions at different taxonomic resolutions were
488 indistinguishable, strongly supporting the view that the necessary reduction in taxonomic resolution
489 applied here has not had a detrimental effect on the potential interpretation of inferred water-table
490 depth profiles from the new model. Indeed, it should be noted that even the highest taxonomic
491 resolution that is practically applicable to light microscopy studies corresponds to a relatively crude

492 resolution in reality given the demonstrated existence of high cryptic and pseudo-cryptic diversity
493 (e.g. Oliverio et al., 2014; Kosakyan et al., 2016), so some degree of taxonomic parsimony will always
494 be necessary.

495

496 *Spatial scales and regional variability*

497 The debate surrounding the degree of cosmopolitanism exhibited in free-living microorganisms, of
498 which testate amoebae provide a good model group, is well established and on-going (e.g. Heger et
499 al., 2009). Conflicting views assume universal ubiquity (Finlay and Clarke, 1999; Finlay et al., 1999,
500 2001) or (occasional) limited geographical distribution of microorganisms (i.e. the 'moderate
501 endemism model'; Foissner, 2008, 2006, 1999). An increasing number of studies focussing on the
502 distribution of testate amoebae have observed taxa which do not appear to support the theory of
503 ubiquity (Smith and Wilkinson, 2007; Smith et al., 2008; Heger et al., 2009, 2011; Yang et al., 2010;
504 Turner et al., 2013; Fournier et al., 2015; Lara et al., 2016).

505

506 Europe possesses relatively few of the physical, climatic and biological barriers typically associated
507 with ecological endemism (Kier et al., 2009) and the passive distribution of testate amoebae should,
508 therefore, be comparatively uninhibited. As a result, it could be argued that any evidence of
509 regionally restricted distributions of testate amoebae in Europe, which cannot be explained by other
510 ecological factors, such as peatland type and trophic status, is supporting evidence of the moderate
511 endemism model.

512

513 By compiling data from across Europe, we were able to examine the distributions of taxa across the
514 continent. The majority (41 of 47) of taxa were found in all regions (Figures 8 and S5), arguing
515 strongly that the continental transfer function can be readily applied to individual core locations
516 within its geographical extent. The Continental region was the most taxonomically diverse, with only
517 *Nebela flabellulum* (strongly skewed to the Atlantic region; Figure 8) completely absent. A similar
518 strongly oceanic distribution has been noted for this taxon in Canadian peatlands (Charman and
519 Warner, 1997), which was the most common to be completely absent from any one region (n=246
520 samples). Three taxa were present only in the Continental region, being completely absent from
521 both the Atlantic and Scandinavian regions (*Centropyxis ecornis* type, *Diffflugia gramen* type,
522 *Paraquadrula irregularis*), however these were rare taxa, with *C. ecornis* type the most common
523 (n=26; Figure 8) and *D. gramen* and *P. irregularis* never occurring >5% in any one sample (n=1 and
524 n=2 respectively). In addition, *P. irregularis* is a calcareous taxon found predominately in rich fens
525 (e.g. Lamentowicz et al., 2013a), which were mainly sampled in the Continental region and were
526 included in the model due to having no associated pH measurement. *Diffflugia labiosa* type was
527 absent from the Atlantic region and present at very low abundance (0.7%) in only one sample in the
528 Scandinavian region. *Arcella hemisphaerica* type was completely absent from the Atlantic region,
529 whereas *Amphitrema wrightianum* type was strongly skewed towards it, also in common with
530 findings from Canada (Charman and Warner, 1997). For nutrient poor, ombrotrophic peatlands,
531 given the number and range of sites included in the dataset, it is likely that these regional patterns
532 represent genuine geographical restrictions of these taxa, rather than a lack of appropriate habitats
533 (Smith and Wilkinson, 2007; Smith et al., 2008; Yang et al., 2010). Patterns relating to taxa
534 commonly associated with other site types (e.g. rich fens; *P. irregularis*, Lamentowicz et al., 2013a)
535 should be viewed with more caution since only limited numbers of geographically restricted samples

536 from such site types were included in the model as a result of their lacking associated pH
537 measurements.

538

539 Twenty-six of 47 taxa showed distributions that were relatively evenly distributed across the three
540 defined eco-regions (Figure S5). These included all of the most common taxa (e.g. *A. muscorum*, *E.*
541 *ciliata* type, *N. tincta* type). Of the taxa shown to have uneven distributions across Europe (Figure 8),
542 the majority (n=14) were found in greater abundance in the taxonomically diverse Continental
543 region. Water table optima of these 14 taxa are evenly distributed (Figure 5) with taxa indicative of
544 wetter (e.g. *Arcella discoides* type, *Arcella vulgaris* type), intermediate (e.g. *Centropyxis arcelloides*
545 type, *Heleopera petricola* type) and drier (e.g. *Bullinularia indica*, *Centropyxis ecornis* type)
546 conditions all represented. In contrast, a much smaller number of taxa had distributions skewed to
547 the Atlantic or Scandinavia regions (Figure 5). Given the similar mean values and water-table depth
548 ranges of all regions, particularly Atlantic and Continental (Table 6; Figure S4), the higher number of
549 taxa skewed to Continental, which include key hydrological indicator taxa commonly found in fossil
550 studies (e.g. *A. discoides* type, *B. indica*) is intriguing. Skewed distributions do not preclude
551 cosmopolitan distributions for many of these taxa, but may relate more to either the general
552 condition or trophic status (e.g Booth and Zygmunt, 2005) of peatlands within each region, or to
553 gradients of oceanicity/continentality. In addition, while differences in the numbers of taxa skewed
554 to particular regions may relate partly to genuine biogeographical differences, they may also be an
555 effect of the different taxonomic knowledge and skill of individual analysts and therefore a reflection
556 of the research design.

557

558 The use of local transfer functions to reconstruct water-table depth from other regions should be
559 approached with caution (Turner et al., 2013), but by including a high number of analogues from a
560 wide geographic region and long water table gradient and by using a relatively coarse taxonomic
561 resolution, we show here that continental-scale models may be just as effective in reconstructing
562 local changes as local-scale models specific to the core data location. A large scale regional model
563 such as that presented here will contain more analogues and therefore provide a more robust
564 approach to reconstructing past hydrological variability than the use of smaller data sets collected
565 from individual sites or small regions.

566

567 *A way forward for interpreting transfer function-based palaeohydrological reconstructions?*

568 Due to the complexity of peatland water table and testate amoeba ecological responses, both
569 moderated by a range of differing factors, it is becoming clear that transfer function reconstructions
570 should not be seen as simple metrics of past climate (Turner et al., 2013). In addition, the apparent
571 inaccuracy of reconstructed water-table depth values, particularly towards the 'dry' end of the
572 gradient where both methodological and ecological problems are exacerbated, suggests that
573 reconstructions should be displayed as residuals or standardised values and interpreted primarily as
574 metrics of directional shifts between wetter and drier conditions, an approach in which context
575 reconstructions from a range of models have shown to be robust (Swindles et al., 2015b). Our own
576 data (e.g. Figures 6 and 7) show that, with some exceptions, our models are relatively consistent in
577 performance for reconstructed water-table depth values across the full gradient. This is likely as a
578 result of the high number of samples characterising all water table segments (Figure S2); although
579 there are relatively fewer samples in drier water table segments, a common problem identified in
580 other studies (Amesbury et al., 2013; Swindles et al., 2015a). Segment-specific n values are still high

581 (lowest is $n=25$ for 45 – 49.5 cm, mean for all water-table depth segments >20 cm is $n=70$),
582 highlighting the value of the large compiled dataset. However, the variability present between both
583 model types and regions, despite an unprecedented training set size, argues that reconstructions
584 should be standardised and presented as residual values (*sensu* Swindles et al., 2015b) in order to
585 focus interpretation on secure directional shifts, avoiding potentially inaccurate conclusions relating
586 to specific water-table depths.

587

588 There has been a recent recognition that testing transfer functions against independent
589 instrumental data may be a more powerful test than relying purely on statistical methods (Swindles
590 et al., 2015b). Here, by applying both approaches, we are able to rigorously validate our new models
591 and show that, despite a low-resolution taxonomic approach, our new pan-European transfer
592 function provides a reliable tool for reconstruction of Holocene hydroclimatic shifts across Europe. In
593 particular, we highlight the potential limitations of applying statistical tests alone. The use of the
594 ‘randomTF’ function, which tests the significance of reconstructions against models trained on
595 randomly generated data has recently been reviewed (Payne et al., 2016), with $>80\%$
596 reconstructions tested found to be insignificant ($p>0.05$), with no correlation between significance
597 and model performance. Our results question the efficacy of this method as different model types
598 applied in different regions (Table 6) showed only 4 out of 12 ‘significant’ reconstructions and
599 resulted in a range of p values from 0.001 to 0.274, despite all reconstructions being trained on the
600 same data and showing what could be interpreted as the same reconstructed patterns of change
601 (Figure 7). Coupled with recent guidance that warns against the use of seemingly arbitrary p -value
602 cut-offs and stresses the need for contextual information in decision making rather than a binary
603 ‘yes/no’ approach (Wasserstein and Lazar, 2016), a multi-faceted approach to model assessment is
604 clearly supported. While statistical validation remains an important and useful indicator of model
605 performance alongside tests against independent data, we advocate a balanced approach to model
606 efficacy taking into account both lines of evidence as well as the role of contextual information. For
607 example, some ‘insignificant’ reconstructions (Table 6) performed well in tests against independent
608 data (Figure 7). In addition, the similarity of reconstructions across model types and/or regions
609 presented here (Figures 6 and 7), despite variations in performance statistics, suggests that the high
610 number of training set samples has resulted in a wider range of modern analogues and therefore a
611 better representation of testate amoeba ecology in the model.

612

613 **Conclusions and guidelines for the application of the transfer function**

614 We developed and validated a new pan-European peatland testate amoeba-based transfer function
615 for palaeohydrological reconstruction using a vastly expanded dataset of 1799 samples and a newly
616 developed low resolution taxonomic scheme to accommodate the large number of data
617 contributors. Following the removal of samples with high pH values, we developed water-table
618 depth transfer functions using a range of model types. These were tested using a combination of
619 statistical validation and comparison to independent test sets with associated instrumental water
620 table measurements. Taxonomic resolution did not impair model performance, which was
621 comparable to other published models. We conclude that the new model provides an effective tool
622 for testate amoeba-based palaeohydrological reconstruction in ombrotrophic peatlands throughout
623 Europe. Model output should be standardised and presented as residual values to focus
624 interpretation on directional shifts and avoiding potential misinterpretation of absolute water-table
625 depth values. The extent and diversity of the dataset highlighted that, at the taxonomic resolution

626 applied, a majority of taxa had broad geographic distributions, though some morphotypes appeared
627 to have restricted ranges.

628

629 To facilitate future research, we provide the full compiled dataset, along with R code to allow the
630 free application of our transfer function to fossil data by individual users, as supplementary online
631 material. The R code facilitates the application of the WA-Tol (inv) model and conversion of
632 reconstructed water-table depth values to standardised residual z-scores. The WA-Tol (inv) model
633 type has been commonly applied in other studies (e.g. Amesbury et al., 2013; Swindles et al., 2015a,
634 2009) and compared favourably to other model types in terms of reported performance statistics in
635 this study. Users are free to alter the R code as appropriate to apply other model types, but should
636 justify these changes in their work.

637

638

639 **Acknowledgements**

640 We gratefully acknowledge and thank all the many landowners and data collectors that have
641 contributed to the large compiled database of European testate amoebae, but who are too
642 numerous to list individually here. This work would not have been possible without them. GTS was
643 supported by the Worldwide University Network ('Arctic Environments, Vulnerabilities and
644 Opportunities') and a Department of Employment and Learning (Northern Ireland) PhD studentship.
645 ET was supported by UK NERC-funded Doctoral Training Grant NE/G52398X/1. ML was supported by
646 EU grant PSPB-013/2010 (CLIMPEAT, www.climpeat.pl) and grant 2015/17/B/ST10/01656 from the
647 National Science Center (Poland). RJP was supported by the Leverhulme Trust (RPG 2015-162). RJP
648 and YM were supported by the Russian Science Foundation (grant 14-14-00891 for field work and
649 grant 14-50-00029 for taxonomic analysis). AB was supported by the RFBR Scientific Fund (grants 16-
650 04-00451A and 15-29-02518) and by the German Ministry of Education and Research (CARBOPERM-
651 Project, BMBF Grant No. 03G0836). EM was supported by the European Community funded BERI
652 project (Bog Ecosystem Research Initiative; ENV4-CT95-0028) and the Swiss Federal Office for
653 Education and Science (95.0415). DJC was supported by the EU ACCROTELM project (EVK2-CT-2002-
654 00166).

655

656 **Figure captions:**

657

658 **Figure 1:** Site locations (see Table 1 for more site details). Sites are coloured by eco-region: Atlantic =
659 red, Scandinavia = green; Continental = blue. For reference to colour, readers are referred to the
660 online version of this article.

661

662 **Figure 2:** Percentage distribution of all taxa. Taxa are ordered from 'wet' on the left to 'dry' on the
663 right based on the taxa optima from the WA-Tol (inv) model of the full dataset (n = 1775).

664

665 **Figure 3:** NMDS plots before (A and B) and after (C and D) the removal of samples from the dataset
666 with high pH values. A and C show sample positions, coded by country. B and D show taxa positions
667 for same data as in A and B (but note different axis lengths). Vectors on all plots show influence of
668 environmental drivers. Some taxa positions in B and D have been marginally altered to improve
669 legibility of the figure, but relative positions remain intact. Full names for species abbreviations can
670 be found in Table 2. For reference to colour, readers are referred to the online version of this article.

671

672 **Figure 4:** Biplots of observed and predicted (leave-one-out cross-validated) water-table depth (left)
673 and residual error plots (right) for the best performing versions of the four model types under
674 investigation. WA-Tol (inv) = weighted averaging with tolerance downweighting and inverse
675 deshrinking; WAPLS C2 = second component of weighted averaging partial least squares; WMAT K5
676 = weighted mean modern analogue technique with five nearest neighbours; ML = maximum
677 likelihood. Red points are model runs with all data, black points are model runs after the removal of
678 samples with high residual values. For reference to colour, readers are referred to the online version
679 of this article.

680

681 **Figure 5:** Water-table depth optima and tolerances (cm) for 57 taxa based on the WA-Tol (inv) model
682 after the removal of outlying samples (n=1302).

683

684 **Figure 6:** Comparison of transfer function reconstructions from four model types (WA-Tol (inv),
685 WAPLS-C2, ML, WMAT-K5) with independent test sets. A, C & E are raw water-table depth values; B,
686 D & F are residual z-scores. A and B: reconstructions from Tor Royal Bog, Dartmoor, UK (Amesbury et
687 al., 2008) compared (panel A only) with a published reconstruction using a European transfer
688 function (black line; Charman et al., 2007). C and D: reconstructions of simulated wet and dry shifts
689 derived from reordered surface samples with associated instrumental water table measurements
690 (black line = annual mean water-table depth, grey line = summer (JJA) mean water-table depth;
691 Swindles et al., 2015b). Y-axis (not shown) is randomly ordered surface sample codes. E and F:
692 reconstructions of near-surface fossil data from Männikjärve Bog, Estonia with associated long-term
693 instrumental water table measurements (black line = annual mean water-table depth, grey line =
694 summer (JJA) mean water-table depth; Charman et al., 2004). For reference to colour, readers are
695 referred to the online version of this article.

696

697 **Figure 7:** Comparison of three regional transfer function reconstructions to the full European model
698 for the same three independent test sets as Figure 6. All reconstructions use the WA-Tol (inv) model
699 type. A: Tor Royal Bog (black line uses the established ACCROTELM European transfer function of
700 Charman et al., 2007); B: simulated changes in water-table depth (black (annual) and grey (summer)
701 lines are instrumental water table measurements); C: Männikjärve Bog, Estonia (black (annual) and
702 grey (summer) lines are instrumental water table measurements). For reference to colour, readers
703 are referred to the online version of this article.

704

705 **Figure 8:** Taxa with uneven distributions across the three regions (n = 19). Taxa with all occurrences
706 < 5% abundance have been excluded (n = 2; DIF GRA and PAR IRR). Region codes on x-axes: Atl. =
707 Atlantic, Scan. = Scandinavia, Cont. = continental Europe. For full taxa abbreviations, see Table 2.
708 Number of occurrences in 1302 samples shown in brackets after taxon code. Red dots indicate
709 complete absence from a particular region. For reference to colour, readers are referred to the
710 online version of this article.

711

712

713 **Supplementary Figure captions:**

714

715 **Figure S1:** NMDS axis 1 scores plotted against pH for all samples (n = 1775). Inset: pH of two k-means

716 cluster analysis groups. Red line in both plots shows cut-off applied of $pH \geq 5.5$.

717

718 **Figure S2:** Sampling distribution for the full dataset ($n=1393$) divided into 12 segments. Lines show
719 segment-wise RMSEP for the best performing versions of the four model types under investigation.
720 Full names for species abbreviations can be found in Table 2 of the manuscript.

721

722 **Figure S3:** Spatial autocorrelation plots for the best performing versions of the four model types
723 under investigation. Full names for species abbreviations can be found in Table 2 of the manuscript.
724 Plots show effect on r^2 by deleting sites at random (open circles), from the geographical
725 neighbourhood of the test site (filled circles) or that are most environmentally similar (crosses)
726 during cross-validation. Note y-axes are on different scales.

727

728 **Figure S4:** Boxplots for water-table depth values for the three regional transfer functions.

729

730 **Figure S5:** Taxa with even distributions across the three regions ($n = 26$). Region codes on x-axes: Atl.
731 = Atlantic, Scan. = Scandinavia, Cont. = continental Europe. For full taxa abbreviations, see Table 2.
732 Number of occurrences in 1302 samples shown in brackets after taxon code.

733

734

735

736 **References**

737 Amesbury, M.J., Charman, D.J., Fyfe, R.M., Langdon, P.G., West, S. 2008. Bronze Age upland
738 settlement decline in southwest England: testing the climate change hypothesis. *Journal of*
739 *Archaeological Science* 35, 87–98.

740 Amesbury, M.J., Mallon, G., Charman, D.J., Hughes, P.D.M., Booth, R.K., Daley, T.J., Garneau, M.
741 2013. Statistical testing of a new testate amoeba-based transfer function for water-table depth
742 reconstruction on ombrotrophic peatlands in north-eastern Canada and Maine, United States.
743 *Journal of Quaternary Science* 28, 27–39.

744 Birks, H.J.B., 1998. Numerical tools in palaeolimnology - Progress, potentialities, and problems.
745 *Journal of Paleolimnology* 20, 307–332.

746 Bobrov, A.A., Charman, D.J. and Warner, B.G. 1999. Ecology of testate amoebae (Protozoa:
747 Rhizopoda) on peatlands in western Russia with special attention to niche separation in closely
748 related taxa. *Protist* 150, 125-136.

749 Booth, R.K. 2008. Testate amoebae as proxies for mean annual water-table depth in Sphagnum-
750 dominated peatlands of North America. *Journal of Quaternary Science* 23, 43–57.

751 Booth, R.K., Zygmunt, J.R. 2005. Biogeography and comparative ecology of testate amoebae
752 inhabiting Sphagnum-dominated peatlands in the Great Lakes and Rocky Mountain regions of North
753 America. *Diversity and Distributions* 11, 577–590.

754 Cash, J. and Hopkinson, J. 1905. *The British Freshwater Rhizopoda and Heliozoa. Volume I.* The Ray
755 Society, London.

756 Cash, J. and Hopkinson, J. 1909. *The British Freshwater Rhizopoda and Heliozoa. Volume II.* The Ray
757 Society, London.

- 758 Cash, J., Wailes, G. and Hopkinson, J. 1915. The British Freshwater Rhizopoda and Heliozoa. Volume
759 III. The Ray Society, London.
- 760 Cash, J., Wailes, G. and Hopkinson, J. 1918. The British Freshwater Rhizopoda and Heliozoa. Volume
761 IV. The Ray Society, London.
- 762 Charman, D.J. and Warner, B.G. 1997. The ecology of testate amoebae (Protozoa: Rhizopoda) in
763 oceanic peatlands in Newfoundland, Canada: modelling hydrological relationships for
764 palaeoenvironmental reconstruction. *Écoscience* 4, 555-562.
- 765 Charman, D.J., Blundell, A. and ACCROTELM members. 2007. A new European testate amoebae
766 transfer function for palaeohydrological reconstruction on ombrotrophic peatlands. *Journal of*
767 *Quaternary Science* 22, 209–221.
- 768 Charman, D.J., Blundell, A., Chiverrell, R.C., Hendon, D. and Langdon, P.G. 2006. Compilation of non-
769 annually resolved Holocene proxy climate records: Stacked Holocene peatland palaeo-water table
770 reconstructions from northern Britain. *Quaternary Science Reviews* 25, 336–350.
- 771 Charman, D.J., Brown, A.D., Hendon, D. and Karofeld, E. 2004. Testing the relationship between
772 Holocene peatland palaeoclimate reconstructions and instrumental data at two European sites.
773 *Quaternary Science Reviews* 23, 137–143.
- 774 Elliott, S.M., Roe, H.M. and Patterson, R.T. 2012. Testate amoebae as indicators of hydroseral
775 change: An 8500 year record from Mer Bleue Bog, eastern Ontario, Canada. *Quaternary*
776 *International* 268, 128–144.
- 777 Finlay, B.J. and Clarke, K.J. 1999. Ubiquitous dispersal of microbial species. *Nature* 400, 1999.
- 778 Finlay, B.J., Esteban, G.F., Clarke, K.J. and Olmo, J.L. 2001. Biodiversity of terrestrial Protozoa appears
779 homogeneous across local and global spatial scales. *Protist* 152, 355–366.
- 780 Finlay, B.J., Esteban, G.F., Olmo, J.L. and Tyler, P.A. 1999. Global distribution of free-living microbial
781 species. *Oikos* 22, 138–144.
- 782 Foissner, W. 1999. Protist diversity: Estimates of the near-imponderable. *Protist* 150, 363–368.
- 783 Foissner, W. 2006. Biogeography and dispersal of micro-organisms: A review emphasizing Protists.
784 *Acta Protozoologica* 45, 111–136.
- 785 Foissner, W. 2008. Protist diversity and distribution: some basic considerations. *Biodiversity and*
786 *Conservation* 17, 235–242.
- 787 Fournier, B., Coffey, E.E.D., van der Knaap, W.O., Fernández, L.D., Bobrov, A. and Mitchell, E.A.D.,
788 2015. A legacy of human-induced ecosystem changes: Spatial processes drive the taxonomic and
789 functional diversities of testate amoebae in Sphagnum peatlands of the Galápagos. *Journal of*
790 *Biogeography* 43, 533–543.
- 791 Hammer, Ø., Harper, D.A.T. and Ryan, P.D. 2001. PAST: Paleontological statistics software package
792 for education and data analysis. *Palaeontologia Electronica* 4, 9pp. [http://palaeo-](http://palaeo-electronica.org/2001_1/past/issue1_01.htm)
793 [electronica.org/2001_1/past/issue1_01.htm](http://palaeo-electronica.org/2001_1/past/issue1_01.htm).
- 794 Heger, T.J., Mitchell, E.A.D., Ledeganck, P., Vincke, S., Van De Vijver, B. and Beyens, L. 2009. The
795 curse of taxonomic uncertainty in biogeographical studies of free-living terrestrial protists: A case
796 study of testate amoebae from Amsterdam Island. *Journal of Biogeography* 36, 1551–1560.

797 Heger, T.J., Booth, R.K., Sullivan, M.E., Wilkinson, D.M., Warner, B.G., Asada, T., Mazei, Y.,
798 Meisterfeld, R. and Mitchell, E.A.D. 2011. Rediscovery of *Nebela ansata* (Amoebozoa : Arcellinida) in
799 eastern North America: biogeographical implications. *Journal of Biogeography* 38, 1897–1906.

800 Heger, T.J., Mitchell, E.A.D., Leander, B.S., 2013. Holarctic phylogeography of the testate amoeba
801 *Hyalosphenia papilio* (Amoebozoa: Arcellinida) reveals extensive genetic diversity explained more by
802 environment than dispersal limitation. *Molecular Ecology* 22, 5172–5184.

803 Jassey, V.E.J., Lamentowicz, L., Robroek, B.J.M., Gąbka, M., Rusińska, A. and Lamentowicz, M. 2014.
804 Plant functional diversity drives niche-size structure of dominant microbial consumers along a poor
805 to extremely rich fen gradient. *Journal of Ecology* 102, 1150-1162.

806 Juggins, S. and Birks, H.J.B., 2011. Quantitative Environmental Reconstructions from Biological Data,
807 in: Birks, H.J.B., Lotter, A.F., Juggins, S., Smol, J.P. (Eds.), *Tracking Environmental Change Using Lake*
808 *Sediments*. Springer Netherlands, Dordrecht, pp. 431–494.

809 Juggins S. 2015. rioja: Analysis of Quaternary Science Data. R package version 0.9–5. [https://cran.r-](https://cran.r-project.org/web/packages/rioja/index.html/)
810 [project.org/web/packages/rioja/index.html/](https://cran.r-project.org/web/packages/rioja/index.html/).

811 Jung, W. 1936. Thekamöben ursprünglicher, lebender deutscher Hochmoore. *Abhandlungen*
812 *Landesmuseum der Provinz Westfalen Museum für Naturkunde* 7, 1–87.

813 Kier, G., Kreft, H., Ming, T., Jetz, W., Ibsch, P.L., Nowicki, C., Mutke, J. and Barthlott, W. 2009. A
814 global assessment of endemism and species richness across island and mainland regions. *PNAS* 106,
815 9322-9327.

816 Kosakyan, A., Lahr, D.J.G., Mulot, M., Meisterfeld, R., Edward, A., Mitchell, D. and Lara, E. 2016.
817 Phylogenetic reconstruction based on COI reshuffles the taxonomy of hyalosphenid shelled testate
818 amoebae and reveals the convoluted evolution of shell plate shapes. *Cladistics*. DOI:
819 10.1111/cla.12167

820 Lamarre, A., Magnan, G., Garneau, M. and Boucher, É. 2013. A testate amoeba-based transfer
821 function for paleohydrological reconstruction from boreal and subarctic peatlands in northeastern
822 Canada. *Quaternary International* 306, 88–96.

823 Lamentowicz, L., Lamentowicz, M. and Gąbka, M. 2008. Testate amoebae ecology and a local
824 transfer function from a peatland in western Poland. *Wetlands* 28, 164-175.

825 Lamentowicz, M. and Mitchell, E.A.D. 2005. The ecology of testate amoebae (Protists) in Sphagnum
826 in north-western Poland in relation to peatland ecology. *Microbial Ecology* 50, 48-63.

827 Lamentowicz, M., Obremaska, M. and Mitchell, E.A.D. 2008. Autogenic succession, land-use change
828 and climatic influences on the Holocene development of a kettle-hole mire in Northern Poland.
829 *Review of Palaeobotany and Palynology* 151, 21-40.

830 Lamentowicz, M., Lamentowicz, L., van der Knaap, W. O., Gąbka, M. and Mitchell, E.A.D. 2010.
831 Contrasting species-environment relationships in communities of testate amoebae, bryophytes and
832 vascular plants along the fen-bog gradient. *Microbial Ecology* 59, 499-510.

833 Lamentowicz, M., Galka, M., Milecka, K., Tobolski, K., Lamentowicz, L., Fialkiewicz-Kozziel, B. and
834 Blaauw, M. 2013a. A 1300-year multi-proxy, high-resolution record from a rich fen in northern
835 Poland: Reconstructing hydrology, land use and climate change. *Journal of Quaternary Science* 28,
836 582–594.

837 Lamentowicz, M., Lamentowicz, L. and Payne, R.J. 2013b. Towards quantitative reconstruction of
838 peatland nutrient status from fens. *The Holocene* 23, 1661-1665.

839 Lamentowicz, M., Słowiński, M., Marcisz, K., Zielińska, M., Kaliszan, K., Lapshina, E., Gilbert, D.,
840 Buttler, A., Fiałkiewicz-Kozieł, B., Jassey, V.E.J., Laggoun-Defarge, F. and Kołaczek, P. 2015.
841 Hydrological dynamics and fire history of the last 1300 years in western Siberia reconstructed from a
842 high-resolution, ombrotrophic peat archive. *Quaternary Research* 84, 312-325.

843 Lara, E., Roussel-Delif, L., Fournier, B., Wilkinson, D.M. and Mitchell, E.A.D. 2016. Soil
844 microorganisms behave like macroscopic organisms : patterns in the global distribution of soil
845 euglyphid testate amoebae. *Journal of Biogeography* 43, 520–532.

846 Li, H., Wang, S., Zhao, H. and Wang, M. 2015. A testate amoebae transfer function from Sphagnum-
847 dominated peatlands in the Lesser Khingan Mountains, NE China. *Journal of Paleolimnology* 54, 189–
848 203.

849 Loeblich, A.R. and Tappan, H. 1961. Remarks on the systematics of the Sarkodina (Protozoa),
850 renamed homonyms and new and validated genera. *Proceedings of The Biological Society of*
851 *Washington* 74, 213-234.

852 Marcisz, K., Lamentowicz, Ł., Słowińska, S., Słowiński, M., Muszak, W. and Lamentowicz, M. 2014.
853 Seasonal changes in Sphagnum peatland testate amoeba communities along a hydrological gradient.
854 *European Journal of Protistology* 50, 445–455.

855 Markel, E.R., Booth, R.K. and Qin, Y. 2010. Testate amoebae and ¹³C of Sphagnum as surface-
856 moisture proxies in Alaskan peatlands. *The Holocene* 20, 463–475.

857 Mazei, Y. A. and Bubnova, O. A. 2007. Species composition and structure of testate amoebae
858 community in a Sphagnum bog at the initial stage of its formation. *Biology Bulletin* 34, 619-628.

859 Mazei, Y. A. and Bubnova, O. A. 2008. Testate amoebae community structure in the Naskaftym
860 Sphagnum bog (middle Volga region). *Povolzhsky Journal of Ecology* 1, 39-47.

861 Mazei, Y. A. and Bubnova, O. A. 2009. Species composition and testate amoebae community
862 structure in pine-Sphagnum bog in northern tundra (Karelia, Russia). *Bulletin of the Moscow Society*
863 *of Naturalists* 114, 15-23.

864 Mazei, Y. A. and Tsyganov, A. N. 2007a. Species composition, spatial distribution and seasonal
865 dynamics of testate amoebae community in Sphagnum bog (middle Volga region, Russia).
866 *Protistology* 5, 156–206.

867 Mazei, Y. A. and Tsyganov, A. N. 2007b. Changes of the testate amoebae community structure along
868 environmental gradients in a Sphagnum-dominated bog under restoration after peat excavation.
869 *Povolzhsky Journal of Ecology* 1, 24 – 33.

870 Mazei, Y. A., Tsyganov, A. N. and Bubnova, O. A. 2007a. Structure of a community of testate
871 amoebae in a Sphagnum dominated bog in upper Sura flow (middle Volga Territory). *Biology Bulletin*
872 34, 382-394.

873 Mazei, Y. A., Tsyganov, A. N. and Bubnova, O. A. 2007b. The species composition, distribution, and
874 structure of a testate amoeba community from a moss bog in the middle Volga river basin.
875 *Zoologicheskyy Zhurnal* 86, 1155-1167.

- 876 Mazei, Y. A., Bubnova, O. A. and Chernyshov, V. A. 2009a. Testate amoebae community structure in
877 a Sphagnum quagmire of a northern tundra bog (Karelia, Russian Federation). Povolzhskiy Journal of
878 Ecology 2, 115-124.
- 879 Mazei, Y. A., Bubnova, O. A., Tsyganov, A. N. and Chernyshov, V. A. 2009b. Species composition and
880 community heterogeneity of testate amoebae within flat Sphagnum quagmire of boggy lake in
881 northern taiga (Karelia, Russia). Izv. Penz. gos. pedagog. univ. im. i V.G. Belinskogo. 14, 64–72.
- 882 Mazei, Y. A., Tsyganov, A. N. and Bubnova, O. A. 2009c. The species composition and community
883 structure of testate amoebae in Sphagnum bogs of northern Karelia (the White Sea lowland).
884 Zoologicheskyy Zhurnal 88, 771-782.
- 885 Mazei, Y. A., Tsyganov, A. N. and Bubnova, O. A. 2009d. The structure of testate amoebae
886 communities in boggy biotopes of the southern taiga (Russian European part). Uspekhi Sovremennoy
887 Biologii 129, 212-222.
- 888 Mazei, Y. A., Bubnova, O. A. and Chernyshov, V. A. 2009e. Community structure of testate amoebae
889 (Testacelobosea; Testacefilosea; Amphitremidae) in Chibirleskoye Sphagnum bog (middle Volga
890 region). Izvestiya Samarskogo Nauchnogo 11, 72-77.
- 891 Meisterfeld, R., 2000a. Testate amoebae with filopodia, in: Lee, J., Leedale, G., Bradbury, P. (Eds.),
892 The Illustrated Guide to the Protozoa, Second Edition. Society of Protozoologists, Lawrence, Kansas,
893 pp. 1054–1084.
- 894 Meisterfeld, R., 2000b. Order Arcellinida Kent, 1980, in: Lee, J., Leedale, G., Bradbury, P. (Eds.), The
895 Illustrated Guide to the Protozoa, Second Edition. Society of Protozoologists, Lawrence, Kansas, pp.
896 827–860.
- 897 Mitchell, E.A.D., Buttler, A. J., Warner, B. G. and Gobat, J-M. 1999. Ecology of testate amoebae
898 (Protozoa: Rhizopoda) in *Sphagnum* peatlands in the Jura mountains, Switzerland and France.
899 Écoscience 6, 565-576.
- 900 Mitchell, E.A.D., Buttler, A.J., Grosvernier, P., Rydin, H., Albinsson, C., Greenup, A., Heijmans, M.,
901 Hoosbeek, M. and Saarinen, T. 2000. Relationships among testate amoebae (Protozoa), vegetation
902 and water chemistry in five *Sphagnum*-dominated peatlands in Europe. New Phytologist 145, 95-
903 106.
- 904 Mitchell, E.A.D., Charman, D.J. and Warner, B.G. 2008. Testate amoebae analysis in ecological and
905 palaeoecological studies of wetlands: Past, present and future. Biodiversity and Conservation 17,
906 2115–2137.
- 907 Mitchell, E.A.D., Payne, R.J., van der Knaap, W.O., Lamentowicz, Ł., Gabka, M. and Lamentowicz, M.
908 2013. The performance of single- and multi-proxy transfer functions (testate amoebae, bryophytes,
909 vascular plants) for reconstructing mire surface wetness and pH. Quaternary Research 79, 6–13.
- 910 Mitchell, E. a D., Lamentowicz, M., Payne, R.J. and Mazei, Y. 2014. Effect of taxonomic resolution on
911 ecological and palaeoecological inference - a test using testate amoeba water-table depth transfer
912 functions. Quaternary Science Reviews 91, 62–69.
- 913 Ogden, C. and Hedley, R. 1980. An atlas of freshwater testate amoebae. Oxford University Press,
914 Oxford.

915 Oksanen, J., Blanchet, F.G., Kindt, R., Legendre, P., Minchin, P.R., Hara, R.B.O., Simpson, G.L.,
916 Solymos, P., Stevens, M.H.H. and Wagner, H. 2015. Package “vegan” version 2.3-1.

917 Oliverio, A.M., Lahr, D.J.G., Nguyen, T. and Katz, L.A. 2014. Cryptic Diversity within Morphospecies of
918 Testate Amoebae (Amoebozoa: Arcellinida) in New England Bogs and Fens. *Protist* 165, 196–207.

919 Payne, R.J. 2010. Testate amoeba response to acid deposition in a Scottish peatland. *Aquatic Ecology*
920 44, 373-385.

921 Payne, R.J., 2011. Can testate amoeba-based palaeohydrology be extended to fens? *Journal of*
922 *Quaternary Science* 26, 15–27.

923 Payne, R.J. and Mitchell, E.A.D. 2007. Ecology of testate amoebae from mires in the central Rhodope
924 Mountains, Greece and development of a transfer function for palaeohydrological reconstruction.
925 *Protist* 158, 159-171.

926 Payne, R.J., Kishaba, K., Blackford, J.J. and Mitchell, E.A.D. 2006. Ecology of testate amoebae
927 (Protista) in south-central Alaska peatlands: building transfer-function models for
928 palaeoenvironmental studies. *The Holocene* 16, 403–414.

929 Payne, R.J., Charman, D.J., Matthews, S. and Eastwood, W.J. 2008. Testate amoebae as
930 palaeohydrological proxies in Sürmeme Ağacbasi Yaylasi peatland (northeast Turkey). *Wetlands* 28,
931 311-323.

932 Payne, R.J., Gauci, V. and Charman, D.J. 2010a. The impact of simulated sulfate deposition on
933 peatland testate amoebae. *Microbial Ecology* 59, 76-83.

934 Payne, R. J., Ryan, P.A., Nishri, A. and Gophen, M. 2010b. Testate amoebae communities of the
935 drained Hula wetland (Israel): implications for ecosystem development and conservation
936 management. *Wetlands Ecology and Management* 18, 177-189.

937 Payne, R.J., Lamentowicz, M. and Mitchell, E.A.D. 2011. The perils of taxonomic inconsistency in
938 quantitative palaeoecology: Experiments with testate amoeba data. *Boreas* 40, 15–27.

939 Payne, R.J., Telford, R.J., Blackford, J.J., Blundell, A., Booth, R.K., Charman, D.J., Lamentowicz, L.,
940 Lamentowicz, M., Mitchell, E.A.D., Potts, G., Swindles, G.T., Warner, B.G. and Woodland, W. 2012.
941 Testing peatland testate amoeba transfer functions: Appropriate methods for clustered training-
942 sets. *The Holocene* 22, 819–825.

943 Payne, R.J., Babeshko, K. V., van Bellen, S., Blackford, J.J., Booth, R.K., Charman, D.J., Ellershaw, M.R.,
944 Gilbert, D., Hughes, P.D.M., Jassey, V.E.J., Lamentowicz, Ł., Lamentowicz, M., Malysheva, E.A.,
945 Mauquoy, D., Mazei, Y., Mitchell, E.A.D., Swindles, G.T., Tsyganov, A.N., Turner, T.E. and Telford, R.J.
946 2016. Significance testing testate amoeba water table reconstructions. *Quaternary Science Reviews*
947 138, 131-135.

948 R Core Team. 2015. R: a language and environment for statistical computing. R Foundation for
949 Statistical Computing: Vienna. <https://www.r-project.org/>.

950 Schönborn, W. 1963. Die Stratigraphie lebender Testaceen im Sphagnetum der Hochmoore.
951 *Limnologica* 1, 315–21.

952 Smith, H.G., Bobrov, A. and Lara, E., 2008. Diversity and biogeography of testate amoebae.
953 *Biodiversity and Conservation* 17, 329–343.

954 Smith, H.G. and Wilkinson, D.M. 2007. Not all free-living microorganisms have cosmopolitan
955 distributions – the case of *Nebela* (Apodera) vs *Certes* (Protozoa : Amoebozoa : Arcellinida). *Journal*
956 *of Biogeography* 34, 1822–1831.

957 Sullivan, M.E. and Booth, R.K. 2011. The potential influence of short-term environmental variability
958 on the composition of testate amoeba communities in Sphagnum peatlands. *Microbial Ecology* 62,
959 80–93.

960 Suzuki, R. and Shimodaira, H., 2014. ‘pvclust’: Hierarchical Clustering with P-Values via Multiscale
961 Bootstrap Resampling. R Package v. 1.3-2. <https://cran.r-project.org/web/packages/pvclust/>.

962 Swindles, G.T., Charman, D.J., Roe, H.M. and Sansum, P. A. 2009. Environmental controls on
963 peatland testate amoebae (Protozoa: Rhizopoda) in the North of Ireland: Implications for Holocene
964 palaeoclimate studies. *Journal of Paleolimnology* 42, 123-140.

965 Swindles, G.T., Blundell, A., Roe, H.M., Hall, V.A. 2010. A 4500-year proxy climate record from
966 peatlands in the North of Ireland: the identification of widespread summer “drought phases”?
967 *Quaternary Science Reviews* 29, 1577–1589.

968 Swindles, G.T., Reczuga, M., Lamentowicz, M., Raby, C.L., Turner, T.E., Charman, D.J., Gallego-Sala,
969 A., Valderrama, E., Williams, C., Draper, F., Honorio Coronado, E.N., Roucoux, K.H., Baker, T. and
970 Mullan, D.J. 2014. Ecology of Testate Amoebae in an Amazonian Peatland and Development of a
971 Transfer Function for Palaeohydrological Reconstruction. *Microbial Ecology* 68, 284–298.

972 Swindles, G.T., Amesbury, M.J., Turner, T.E., Carrivick, J.L., Woulds, C., Raby, C., Mullan, D., Roland,
973 T.P., Galloway, J.M., Parry, L.E., Kokfelt, U., Garneau, M., Charman, D.J. and Holden, J. 2015a.
974 Evaluating the use of testate amoebae for palaeohydrological reconstruction in permafrost
975 peatlands. *Palaeogeography, Palaeoclimatology, Palaeoecology* 424, 111–122.

976 Swindles, G.T., Holden, J., Raby, C.L., Turner, T.E., Blundell, A., Charman, D.J., Menberu, M.W. and
977 Kløve, B. 2015b. Testing peatland water-table depth transfer functions using high-resolution
978 hydrological monitoring data. *Quaternary Science Reviews* 120, 107–117.

979 Telford, R.J. and Birks, H.J.B. 2005. The secret assumption of transfer functions: Problems with
980 spatial autocorrelation in evaluating model performance. *Quaternary Science Reviews* 24, 2173–
981 2179.

982 Telford, R.J. and Birks, H.J.B., 2009. Evaluation of transfer functions in spatially structured
983 environments. *Quaternary Science Reviews* 28, 1309–1316.

984 Telford, R.J. and Birks, H.J.B. 2011a. A novel method for assessing the statistical significance of
985 quantitative reconstructions inferred from biotic assemblages. *Quaternary Science Reviews* 30,
986 1272–1278.

987 Telford, R.J. and Birks, H.J.B. 2011b. Effect of uneven sampling along an environmental gradient on
988 transfer-function performance. *Journal of Paleolimnology* 46, 99–106.

989 Telford, R. J. 2015. palaeoSig: Significance Tests for Palaeoenvironmental Reconstructions. R package
990 version 1.1-3. <https://cran.r-project.org/web/packages/palaeoSig/>.

991 Tolonen, K. Warner, B. G. and Vasander, H. 1992. Ecology of Testaceans (Protozoa, Rhizopoda) in
992 Mires in Southern Finland .1. Autecology. *Archiv fur Protistenkunde* 142, 119-138.

993 Tsyganov, A. N. and Mazei, Y. A. 2007. The species composition and structure of testate amoebae
994 community in a bogged lake in the middle Volga basin. *Uspekhi Sovremennoĭ Biologii* 127, 305-315.

995 Turner, T.E., Swindles, G.T., Charman, D.J. and Blundell, A. 2013. Comparing regional and supra-
996 regional transfer functions for palaeohydrological reconstruction from Holocene peatlands.
997 *Palaeogeography, Palaeoclimatology, Palaeoecology* 369, 395–408.

998 van Bellen, S., Mauquoy, D., Payne, R.J., Roland, T.P., Daley, T.J., Hughes, P.D.M., Loader, N.J., Street-
999 Perrott, F.A., Rice, E.M. and Pancotto, V.A. 2014. Testate amoebae as a proxy for reconstructing
1000 Holocene water table dynamics in southern Patagonian peat bogs. *Journal of Quaternary Science* 29,
1001 463–474.

1002 van Breemen, N. 1995. How Sphagnum bogs down other plants. *Trends in Ecology and Evolution* 10,
1003 270–275.

1004 Warner, B. G. and Charman, D. J. 1994. Holocene soil moisture changes on a peatland in
1005 northwestern Ontario based on fossil testate amoebae (Protozoa) analysis. *Boreas* 23, 270-279.

1006 Wasserstein, R.L. and Lazar, N.A. 2016. The ASA’s statement on p-values: context, process, and
1007 purpose. *The American Statistician* 70, 129-133.

1008 Willis, K.S., Beilman, D., Booth, R.K., Amesbury, M., Holmquist, J. and MacDonald, G. 2015. Peatland
1009 paleohydrology in southern West Siberian Lowlands: Comparison of multiple testate amoeba
1010 transfer functions, sites, and Sphagnum ¹³C values. *The Holocene* 25, 1425-1436.

1011 Woodland, W.A., Charman, D.J. and Sims, P.C., 1998. Quantitative estimates of water tables and soil
1012 moisture in Holocene peatlands from testate amoebae. *The Holocene* 8, 261–273.

1013 Yang, J., Smith, H.G., Sherratt, T.N. and Wilkinson, D.M. 2010. Is there a size limit for cosmopolitan
1014 distribution in free-living microorganisms? A biogeographical analysis of testate amoebae from polar
1015 areas. *Microbial Ecology* 59, 635–645.

1016

1017

1018

1019

1020

1021

1022

1023

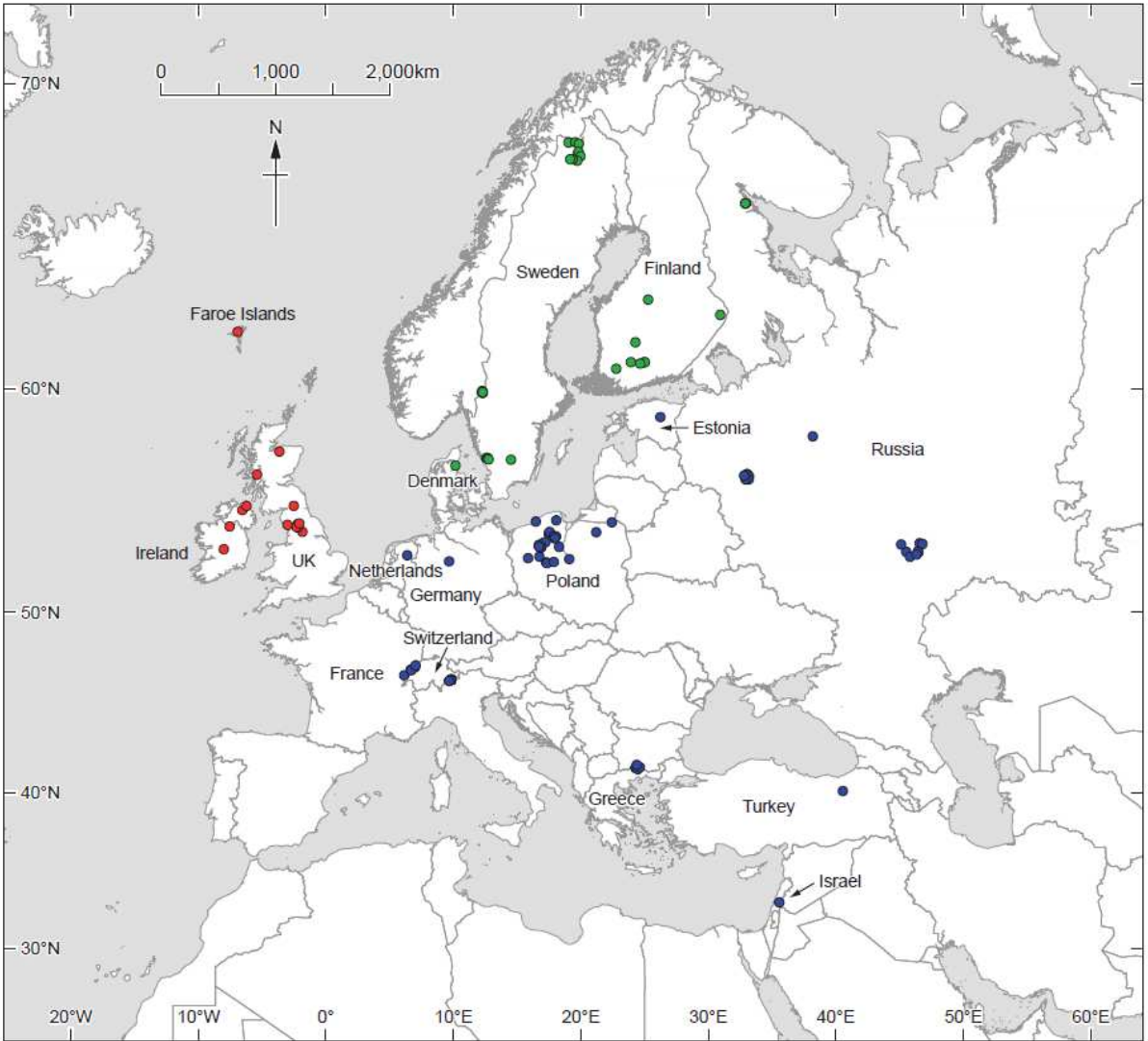
1024

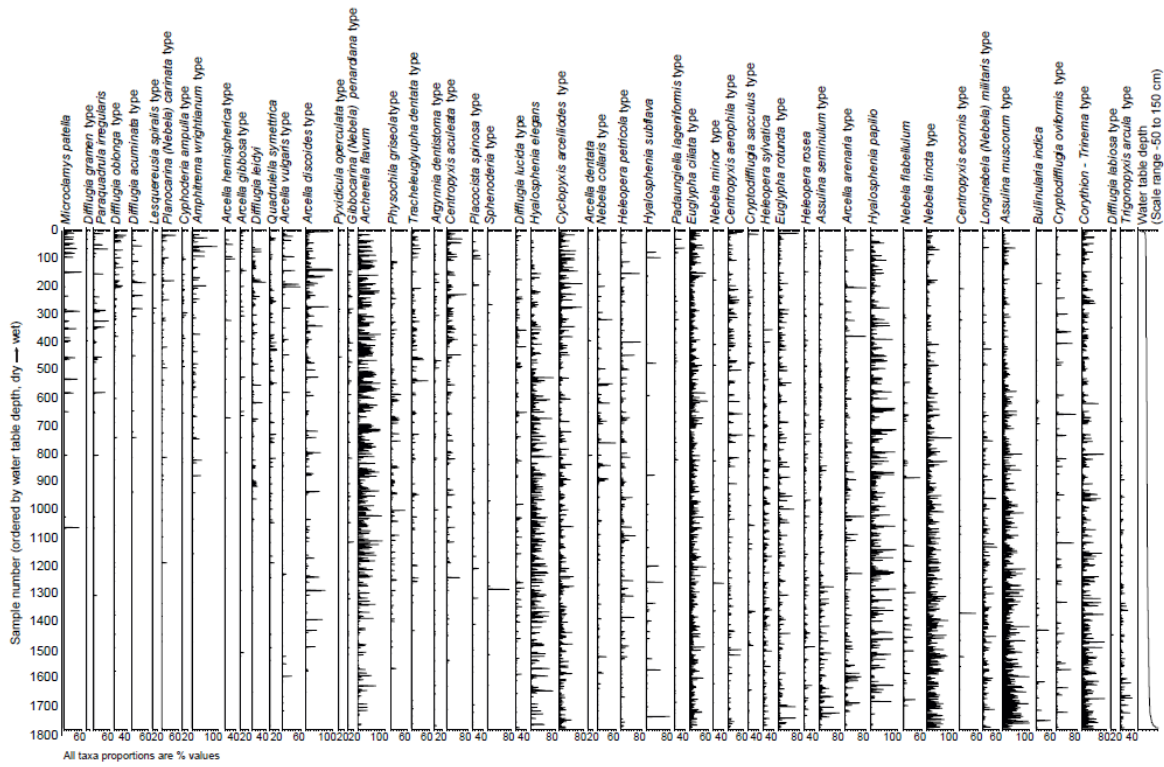
1025

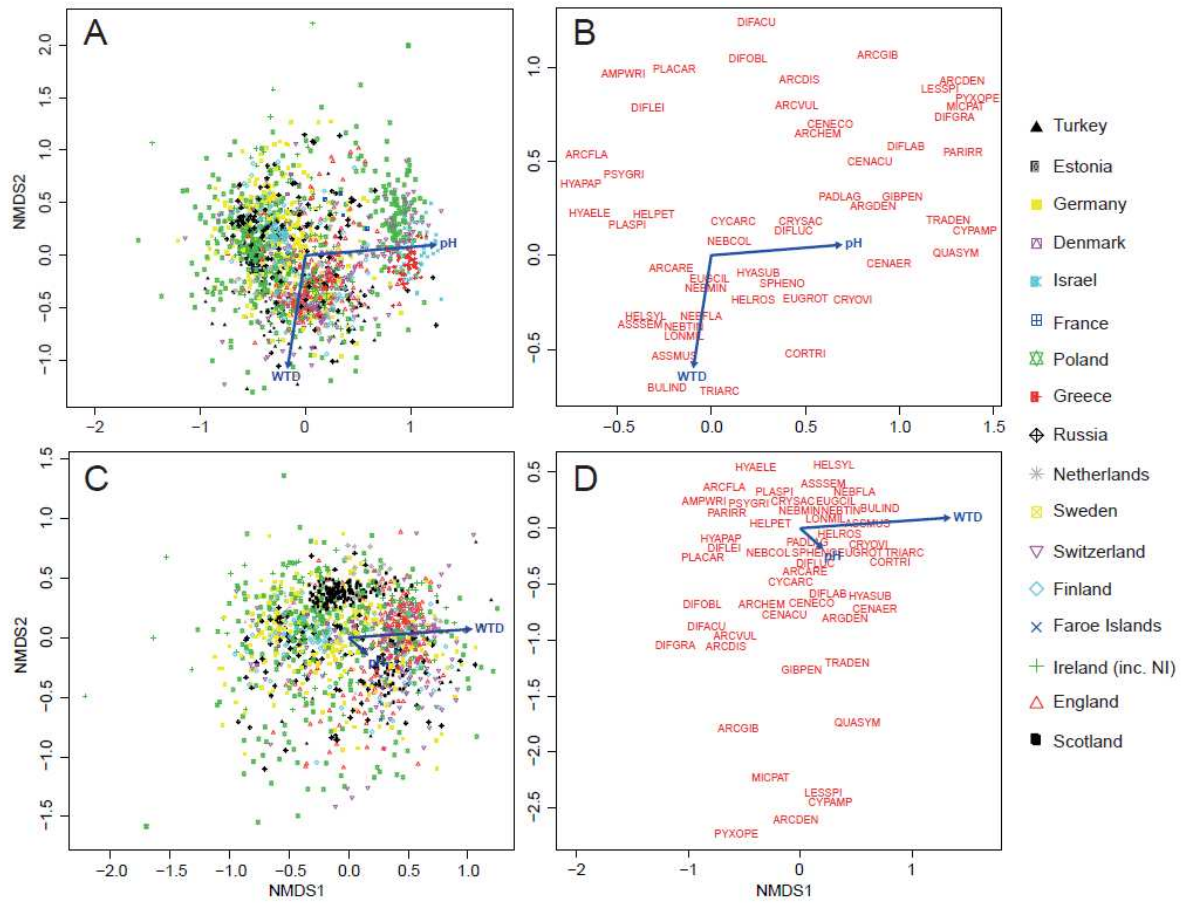
1026

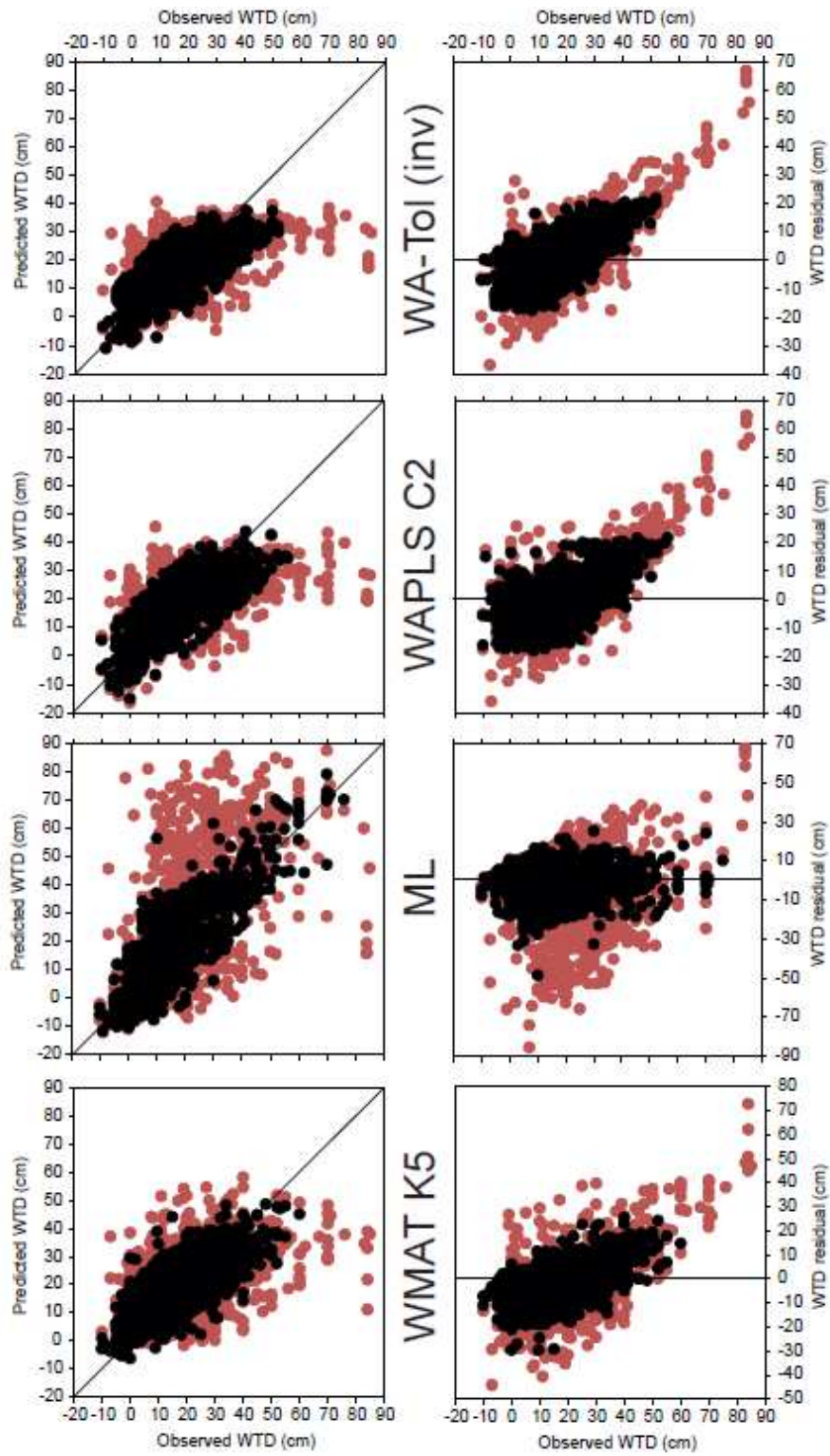
1027

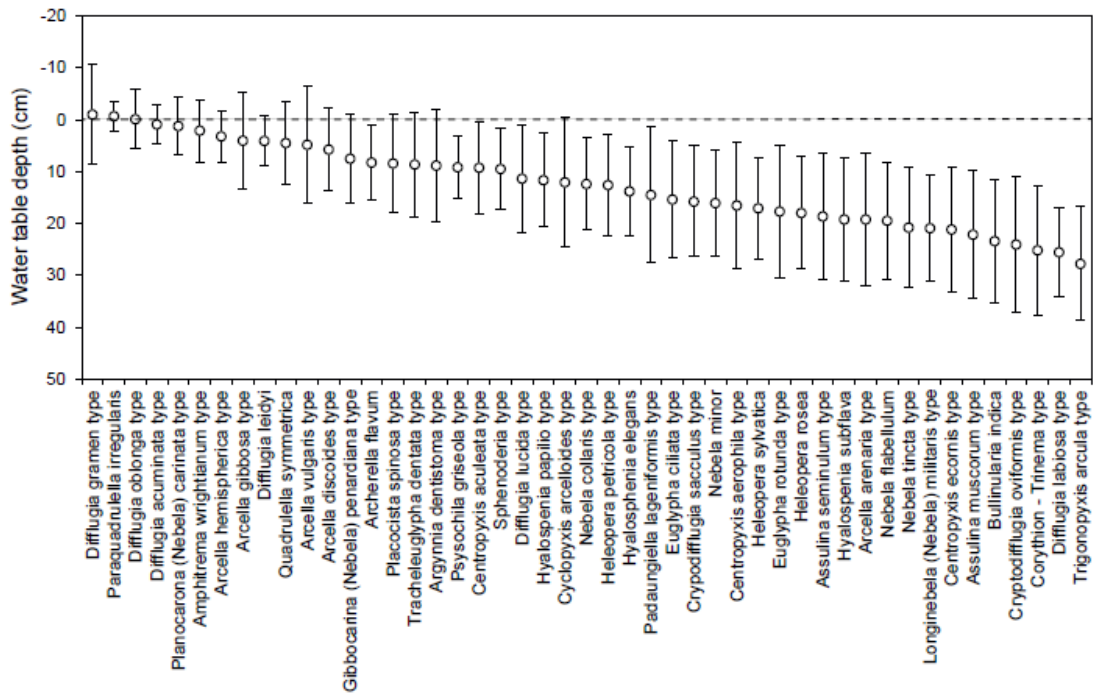
1028



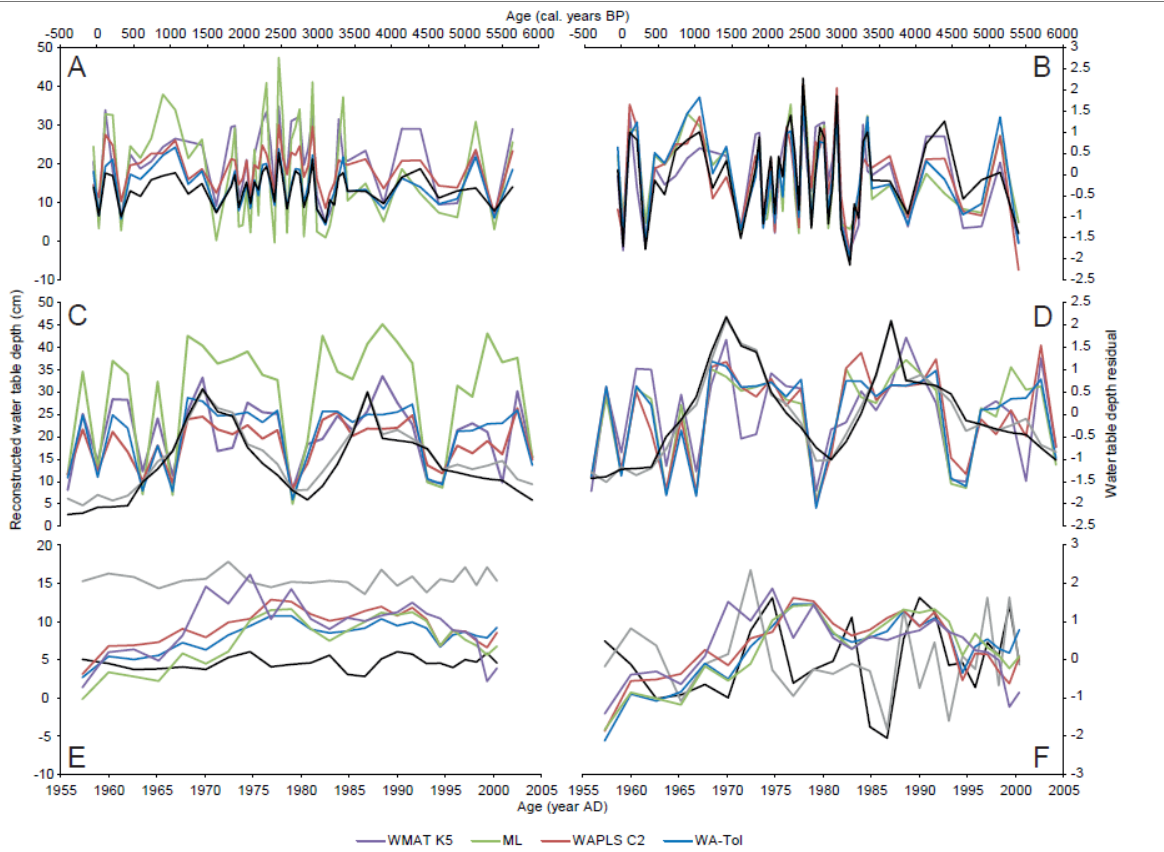








1033



1034

